Available online at www.sciencedirect.com

ScienceDirect

Ceramics International 40 (2014) 683–689

CERAMICS INTERNATIONAL

www.elsevier.com/locate/ceramint

Microstructure, mechanical properties, and bonding mechanism of ultrasonic-assisted brazed joints of SiC ceramics with ZnAlMg filler metals in air

Xiaoguang Chen, Jiuchun Yan*, Sichao Ren, Qian Wang, Jinghui Wei, Guohua Fan

State Key Laboratory of Advanced Welding and Joining, Harbin Institute of Technology, Harbin 150001, PR China

Received 5 March 2013; received in revised form 15 June 2013; accepted 16 June 2013
Available online 21 June 2013

Abstract

SiC ceramic samples were brazed to each other in air using ultrasonic-assisted brazing, filling with ZnAlMg alloys at 420 °C. The microstructure, mechanical properties, and interfacial bonding mechanism of the joint were investigated. The ultrasonic vibration duration time (UVDT) significantly affected the strength of the joint. A joint with a high strength of ~148 MPa was obtained when the UVDT was increased to 8 s. An amorphous SiO_2 film with a thickness of ~6 nm was formed on the surface of SiC during heating in air. When ultrasonically vibrated, the liquid ZnAlMg filler metal eroded the SiO_2 film nonuniformly. This erosion behavior was induced by the impact from liquid micro-jets, shock waves, and localized high temperatures, all of these effects being ascribed to the implosion of the cavitation bubble. The atoms generated from the erosion of the SiO_2 film diffused away quickly in the liquid alloy, aided by the acoustic streaming effect. This erosion behavior belonged to a special phenomenon of cavitation erosion. Other amorphous phases not eroded by the liquid ZnAlMg alloy were preserved at the final interface. Strong bonding between the SiC and the ZnAlMg filler metal could be ascribed to cavitation erosion-induced mass transfer from SiO_2 to ZnAlMg; this mass transfer behavior was enhanced by prolonging the UVDT.

Keywords: A. Joining; B. Interfaces; C. Mechanical properties; D. SiC

1. Introduction

Bonding metals to silicon carbide (SiC) ceramics is of fundamental interest for fabricating complex-shaped SiC components by brazing, and for brazing SiC-reinforced aluminum metal matrix composites (SiCp/Al MMCs) with a high volume fraction of reinforcements, because of the existence of plentiful SiC particles on the composite surface. To our knowledge, the wettability of common metals or alloys to SiC ceramics is very poor. This problem can be overcome by using activated filler metals [1,2], where an active element (e.g. titanium) destabilizes the ionic or covalent bonding of the ceramic and alters the surface chemistry of the ceramic by forming an intermediate reaction layer. Liu et al. [3] used a common Ag–35.25Cu–1.75Ti (wt%) filler metal to join SiC ceramics and a higher flexural strength of ~342 MPa was achieved at 900 °C for 30 min. Lee et al. [4] brazed SiC ceramics by use of the Ag–5Ti (at%) filler metals, and the joints with high flexural strength of ~178 MPa were brazed at 985 °C for 10 min. A new Co-based alloy with complex components (Co, Fe, Ni, Cr, Ti, Si, and B) was developed by Xiong et al. [5,6], which provided a four-point bend strength of ~161 MPa for SiC/SiC joint brazed at 1150 °C for 10 min. Riccardi et al. [7] used the Ti–84Si (at%) alloys for the joining of SiC_f/SiC composites, and the joints brazed at 1330 °C for 10 min showed a shear strength of ~71 MPa. Li et al. [8,9] used the Ti–78Si (wt%) alloys for the joining of SiC ceramics, and the joints brazed at 1400 °C for 10 min showed

*Corresponding author. Tel.: +86 451 86418695; fax: +86 451 86416186.
E-mail addresses: xgchenhit@126.com (X. Chen), jcyan@hit.edu.cn (J. Yan).

0272-8842/$ - see front matter © 2013 Elsevier Ltd and Techna Group S.r.l. All rights reserved.
http://dx.doi.org/10.1016/j.ceramint.2013.06.055

shear strength of ~125 MPa. Ni–50Ti (at%) alloy with a high melting temperature was adopted to join SiC ceramics by Naka et al. [10], and the joint brazed at 1600 °C for 30 min could reach a shear strength of ~154 MPa. Majority of the filler metals designed for joining SiC ceramics were focused on the high temperature application of joints. However, the aluminum matrix of SiCp/Al MMCs cannot tolerate such high brazing temperatures, so decreasing the brazing temperature of SiC ceramics is important for joining composites, and helps to relax the thermal stresses present in brazed joints of pure SiC ceramics [11].

Some researchers have tried to join ceramics by brazing at low temperatures. Various Sn-based activated alloys with melting temperatures below 300 °C have been explored as filler metals for the brazing of ceramic materials [11,12]. Unfortunately, high temperatures above ~800 °C were usually needed during the brazing process, which allowed for the thermodynamic driving force to start chemical reactions between the active element and ceramic. Ultrasonic vibration can assist in the brazing process by adding energy to the system, significantly improving the wettability of the liquid to the solid [13–16]. Naka et al. [15,16] introduced ultrasonic vibration while dipping ceramics in a molten Zn-based alloy solution, and also while ultrasonic-assisted brazing metallized ceramics to metals by filling with the same Zn-based alloys at 400–500 °C. Ultrasonic vibration duration time (UVDT) showed significant effects on the joint strength, and the shear strength of SiC/Cu joints could reach to ~78 MPa for a UVDT of 90 s. Recently a similar Zn-based filler metal was used for ultrasonic-assisted brazing of SiCp/Al MMCs with a volume fraction of ~55% [17]. However, the bonding mechanism of Zn-based alloys to SiC ceramics under ultrasonic vibration is not clearly understood. In this study, SiC ceramics were ultrasonic-assisted brazed to each other by filling with Zn-based filler metals at 420 °C in air. We explored the effects of the UVDT on the microstructure and mechanical performance of the joints, as well as the interfacial bonding mechanism of the joint.

2. Experimental procedure

The SiC ceramic used in this investigation was made by pressureless sintering, creating 40 mm × 10 mm × 3 mm samples of ~99% purity. Its surface was then polished using diamond paste with a 1 μm grit size. Zn–8.5Al–1Mg (wt%) alloys used as filler metals were prepared by melting pure metals (Zn, Al, and Mg) in a medium-frequency induction furnace with an argon atmosphere. The polished substrate and the prepared filler metals were ultrasonically cleaned in acetone for 15 min before the joining process.

A self-assembled ultrasonic-assisted brazing system equipped with an electric resistance-heated furnace was used in the experiment. The ultrasonic equipment comprises an ultrasonic generator, an ultrasonic transducer, and a 20 mm diameter titanium alloy horn. The ultrasonic transducer was cooled by circulating water to ensure stability of the ultrasonic vibrations. The ultrasonic vibration had a frequency of 20 ± 0.1 kHz. The amplitude of the ultrasonic vibration was ~3.5 μm, which was measured by a laser doppler vibrometer (Polytec OFV-505/5000, Germany). The vibrometer used the heterodyne interferometer principle to acquire the characteristics of mechanical vibrations according to the following formula:

$$A = \int_0^{T/4} \nu \sin\ \omega t dt = \int_0^{\pi/4} \frac{\nu}{\omega} \sin(\omega t) d(\omega t) = \frac{\nu}{\omega} = \frac{\nu}{2\pi f} \tag{1}$$

where A is the amplitude, T is the period of the sine wave, ν is the vibration velocity, ω is the palstance, and f is the frequency.

A schematic of the ultrasonic-assisted brazing process is shown in Fig. 1. The processed SiC samples were placed in a single overlap configuration with a ~20 mm overlapped length. The samples were then heated to 420 °C in air. An ultrasonic vibration was applied to the lower plate, having an amplitude of ~3.5 μm, a frequency of 20 kHz, and a varying of UVDT of 2 s, 4 s, 8 s, or 16 s. The joined sample was then allowed to naturally cool in the furnace.

The state of the SiC surface that experienced only thermal treatment (420 °C) was determined by X-ray photoelectron spectroscopy (XPS, PHI 5700 ESCA). The phase composition of the filler metal was identified using X-ray diffraction (XRD, X'Pert PW3040). The solidus and liquidus temperatures of the filler metal were determined by differential thermal analysis (DTA) tests. A cross section of the joint was prepared by standard polishing techniques. The microstructures of the prepared filler metals and joints as well as the morphologies of the fracture surfaces were observed using a scanning electron microscope (SEM, FEI Quanta 200 F) equipped with an energy-dispersive X-ray spectrometer (EDS). High-resolution transmission electron microscopy (HRTEM, FEI Tencnai G^2F30) was used to identify the detailed interfacial microstructure. Specimens for HRTEM were prepared using a focused ion beam (FIB, FEI HELIOS NanoLab 600i). Three specimens for shear tests were cut from the original joints; each sample was 5 mm × 10 mm × 6 mm with a joint area of ~50 mm^2. Shear strength was evaluated in an electronic tension testing machine (Instron 5569) at a constant displacement rate of 0.5 mm/min.

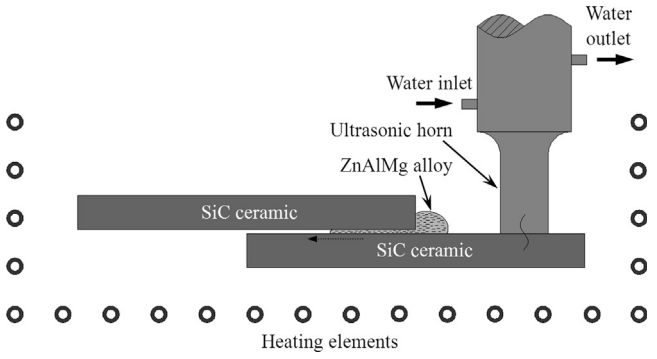

Fig. 1. Schematic of the ultrasonic-assisted brazing process.

3. Results and discussion

The nonequilibrium microstructure of the prepared ZnAlMg alloy consists of an β-Zn phase (white), an α-Al phase (black), and a Zn–Al–Mg eutectic phase (textured pattern) (Fig. 2a). Based on XRD analysis, The phase compositions in the prepared alloy are Zn phases, Al phases, and intermetallic compound $MgZn_2$ phases (Fig. 2b). According to EDS results (Table 1), the $MgZn_2$ phases usually exist in the eutectic zones because of the higher concentration of Mg in the eutectic phases. The solidus (T_S) and liquidus (T_L) temperature of the ZnAlMg alloy are about 371.5 °C and 394.5 °C (Fig. 2c), respectively.

With ultrasonic vibration applied to the lower plate, the liquid ZnAlMg alloy quickly filled the joint clearance to form an integrated joint. This result is consistent with that of our previous study [18,19]. Varying the UVDT does not change the microstructure of the joint; a representative joint is shown in Fig. 2d. The interface between the filler metal and the base metal is continuous, and the joint area is free of pores. Although the compositions of the phases in the joint alloy are consistent with those in the original casting filler metal (Table 1), their morphologies exhibit some changes (Fig. 2d). Many tiny textured patterns appear in the joint Al phase, caused by precipitation of a β-Zn phase in the Al phase from a eutectoid reaction [20,21]. The eutectic phase becomes coarser than that in the original filler metals. These differences could be ascribed to the slower cooling rate after the brazing process. Usually, the eutectic phase and Zn phase exist adjacent to the interface, with no Al phases directly contacting the SiC ceramic. When viewed using an SEM, the interface appears to be relatively sharp, and obvious chemical reaction, dissolution, or diffusion is not present (Fig. 2e). A gray phase with a chemical composition (Table 1) similar to the stoichiometric $MgZn_2$ phase formed at the local interface.

Fig. 3 shows the relationship between the shear strength of the joint and the UVDT used. To obtain the accurate and steady strength values, six samples were used in the shear test

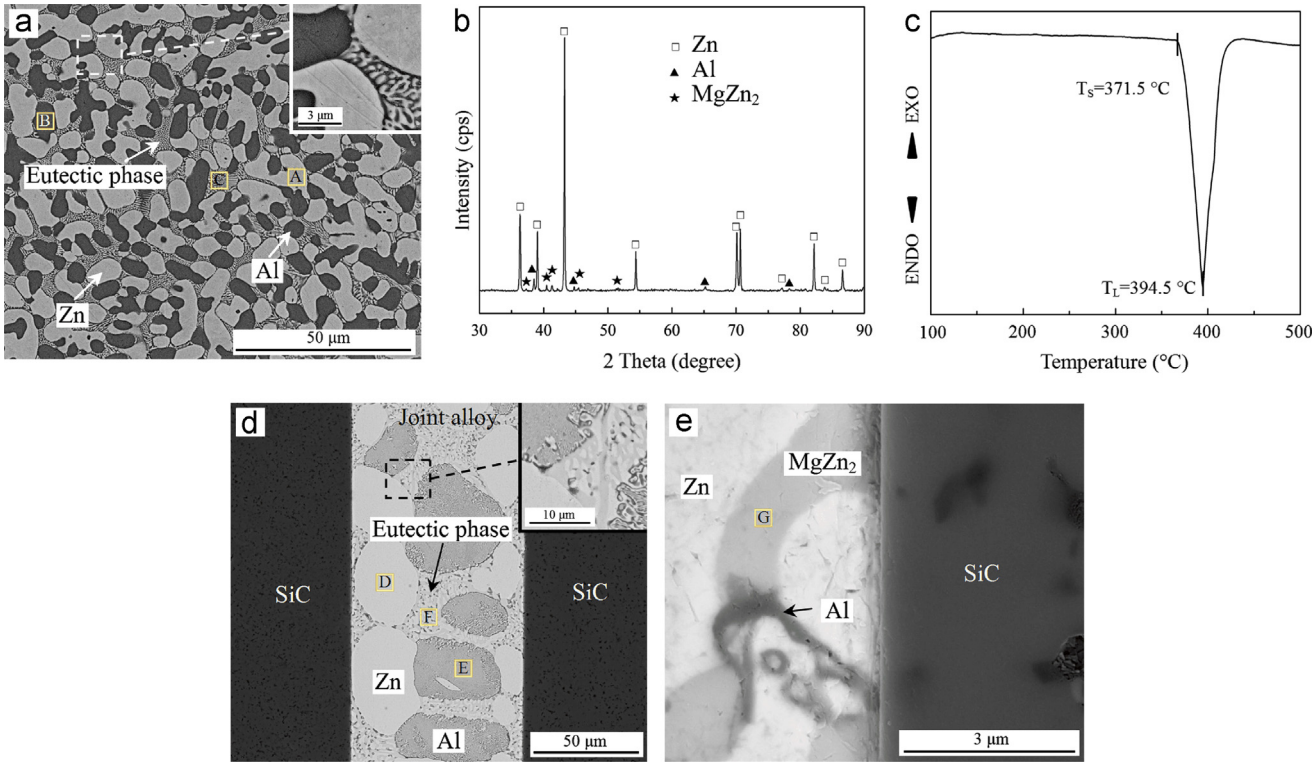

Fig. 2. (a) Microstructure, (b) XRD, and (c) DTA analysis of the prepared filler metal; microstructure of (d) the joint and (e) the corresponding interface.

Table 1
EDS results for the different zones indicated in Figs. 2 and 4.

Element (at%)	Zones											
	A	B	C	D	E	F	G	H	I	J	K	L
Zn	96.96	62.43	80.09	97.11	56.42	78.35	62.93	97.35	78.91	58.49	96.43	76.29
Al	2.55	37.24	9.00	2.15	43.33	14.50	1.63	2.37	13.07	41.14	3.41	13.16
Mg	0.49	0.33	10.91	0.67	0.25	7.15	35.45	0.28	8.02	0.37	0.16	9.55
Phase	Zn	Al	Eutectic phase	Zn	Al	Eutectic phase	$MgZn_2$	Zn	Eutectic phase	Al	Zn	Eutectic phase

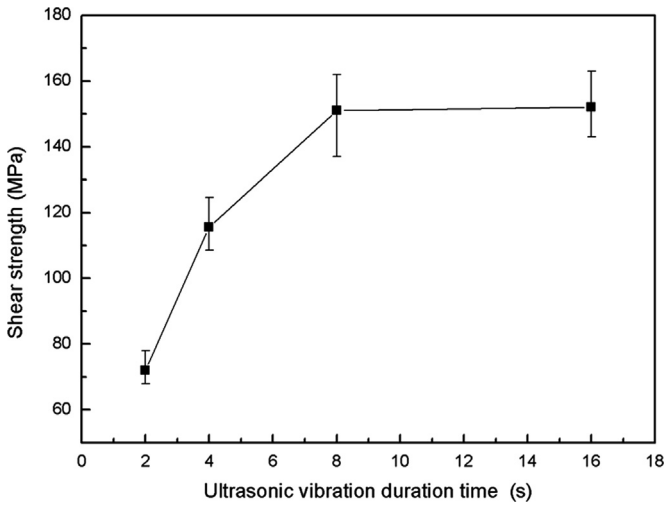

Fig. 3. Change of the joint shear strength with a varying UVDT.

for each UVDT. The shear strength increases as the UVDT lengthens. A high shear strength of ~148.1 MPa is achieved at a UVDT of 8 s, which has been confirmed by repeated experiments. Further increasing the UVDT does not significantly improve the joint strength. The strength value is close to the results of Ref. [10], but a significant weakness is that the service temperature of joints is very limited due to the low melting temperature of ZnAlMg filler metals.

Schematic of fracture paths and morphology of fracture surfaces of the joints obtained with different ultrasonic vibration duration times

Fig. 4 shows schematic of fracture paths and morphology of fracture surfaces of the joints brazed with varying UVDTs. When the UVDT is 2 s, the joint strength is low. Fracture path usually occurs at the interface between the filler metal and SiC ceramic, and fracture of the joint alloy is partially caused by torsion during the shear process (Fig. 4a). This indicates that the bonding interfaces are the weak zones for the short UVDT joints. According to EDS (Table 1) analysis and the morphology of the fracture surface in the joint alloy, the Zn phase and eutectic phase exhibit brittle failure, whereas the dimples appearing on the Al phase suggest a ductile rupture mechanism (Fig. 4c). For the highest strength joints, the fracture surfaces indicate that failure mainly occurs in three zones: the interface, the interior of the SiC, and within the joint alloy (Figs. 4b and d). Cracks in the joint alloy usually exist near the interface, confirmed by the lack of Al phases on the corresponding fracture surface according to EDS (Table 1). This behavior can be ascribed to the excellent toughness of the Al phases compared with the brittle Zn and eutectic phases. The UVDT can have obvious effects on the shear strength of the joint, because a strong bonding interface forms between the ZnAlMg filler metal and SiC ceramic when the UVDT is enough long. It is plausible that the ultrasonic vibration changes the interfacial structure gradually as UVDT is changed.

HRTEM was used to investigate the characteristics and structure of the interface (Fig. 5a). The phases adjacent to the interface identified by selected area diffraction patterns (SADP) are hcp Zn (Fig. 5b) and hcp 6H–SiC (Fig. 5c). An amorphous layer is observed between the Zn phase and SiC phase. The interface between the amorphous layer and SiC phase is relatively smooth, but the interface between the amorphous layer and Zn phase is very rough. The minimum and maximum thicknesses of the amorphous layer are ~2 nm and ~6 nm, respectively.

Because the SiC ceramics were bonded with a ZnAlMg filler metal that formed an interfacial amorphous layer, understanding the formation of this layer is essential for analyzing the bonding mechanism. It is difficult to quantify the composition of the amorphous layer because of its thinness. It is known that an oxide film, usually amorphous, can form on the SiC surface when heated in air. The surface of the SiC sample that experienced only thermal treatment (420 °C) was checked in HRTEM. An amorphous layer with a thickness of ~6 nm forms on the SiC surface (Fig. 6). The surface of the same sample was also investigated with XPS. The components of the Si 2p line at binding energies of ~100 eV and ~102.5 eV represent the SiC and SiO_2 fractions on the SiC surface, respectively (Fig. 7). These results indicate that an amorphous SiO_2 layer forms on the SiC surface in the absence of ultrasonic interactions with the ZnAlMg filler metal. This amorphous layer is likely the original SiO_2 film grown on the SiC surface during heating in air, supported by the observation that it has the highest thickness and a smooth interface with SiC after brazing.

The SiO_2 film on the SiC surface was bonded well with the ZnAlMg filler metal when ultrasonic vibration was applied. The rough interface observed between the filler metal and SiO_2 layer in this case suggests that the SiO_2 film partially dissolved into the liquid ZnAlMg filler metal, and that this dissolution behavior was not uniform over the whole interface. These results indicate that the local environment at the interface between the liquid ZnAlMg alloy and the solid SiO_2 film is not consistent. Variation in the local environment can be ascribed to ultrasonic effects, which are primarily caused by acoustic cavitation in the liquid filler metal. Acoustic cavitation is the formation, growth, and rapid implosive collapse of microbubbles. Rapid bubble implosion can induce a tiny hot spot. The localized temperature and pressure inside the bubble are estimated to be about 5000 K and 0.1 GPa, respectively. [22,23]. The effective temperature of the liquid surrounding the bubble can reach 1600 °C [23]. Even though the temperature is extraordinarily high, the region itself is so small that the heat dissipates quickly. Thus, it is believed that only the bubbles imploding adjacent to the interface can affect the solid surface. When a bubble is close to a solid boundary, its implosion becomes asymmetric because of pressure distortion from the boundary. This distortion leads to a special phenomenon: an inrush of liquid passes through the bubble, penetrates the opposite bubble interface, and strikes the solid surface with high velocity. In addition, the collapse of the bubble leads to the emission of a shock wave. The liquid micro-jet, shock wave, and localized high temperature may only last a few microseconds, but these effects can damage the solid surface. This phenomenon is known as cavitation erosion [24]. Many

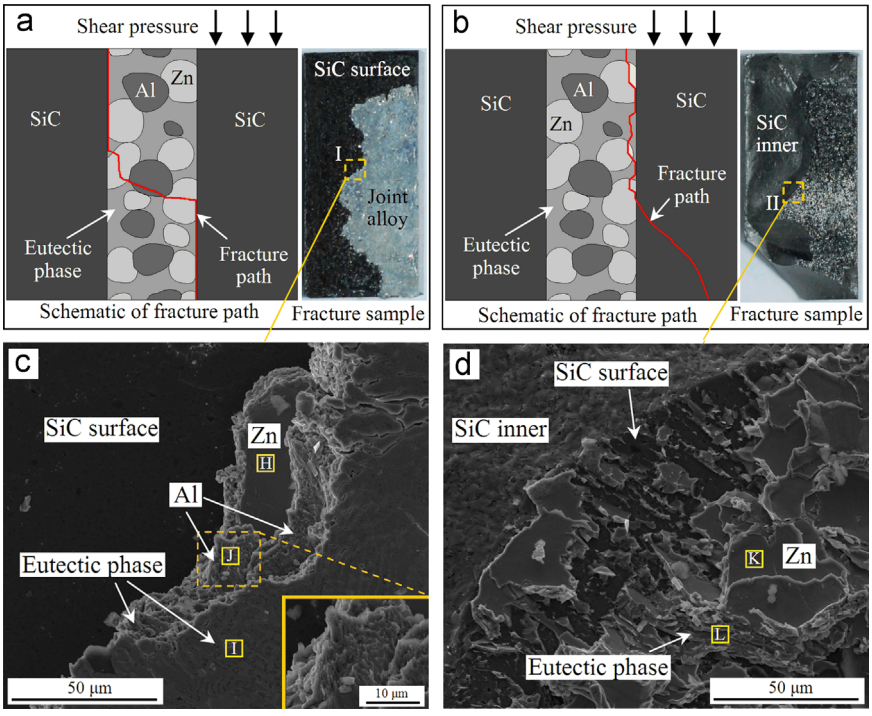

Fig. 4. Schematic of fracture paths and morphology of fracture surfaces of the joints obtained with different ultrasonic vibration duration times of (a) and (c) 2 s, (b) and (d) 8 s. (The (c) and (d) are the local magnification images of the corresponding quadrate areas I in (a) and II in (b), respectively).

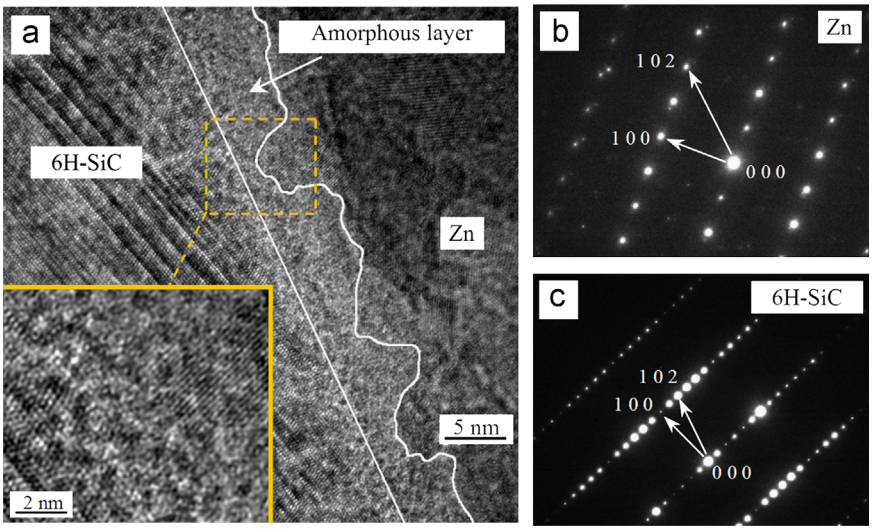

Fig. 5. (a) HRTEM image of the interface between SiC and ZnAlMg for a UVDT of 8 s; (b) SADP of SiC; and (c) SADP of Zn.

researchers [24–27] have found that a variety of materials (glasses, ceramics, metals, and alloys) can be eroded using a water solution vibrated by an ultrasonic treatment for long periods of time (few tens of minutes), and that the erosion extent increases with an increasing UVDT.

The erosion process of the SiO_2 film by the liquid ZnAlMg filler metal is difficult to observe directly. One possible explanation for the erosion process is that a redox reaction can occur between the Al or Mg in the filler metal and the SiO_2 film, producing a corresponding metal oxide and Si. However, these reaction products are not observed in this study. According to reports [28,29], reactions between Al or Mg and SiO_2 do not easily occur for such a short time and low temperature. A previous study on the ultrasonic-assisted interaction between liquid Al–Si and solid Ti–6Al–4 V showed that cavitation erosion could intensely affect interfacial interactions in localized areas [30]. The nonuniform dissolution behavior in this study could also be ascribed to cavitation erosion. The liquid micro-jets, shock waves, and localized high temperatures during the implosion of bubbles adjacent to the interface could cause the SiO_2 film near the bubbles to decompose directly into the liquid filler metal.

The acoustic streaming effect, an additional phenomenon induced by ultrasonic vibration, must also be considered because it can accelerate the movement of atoms in the liquid ZnAlMg alloy. The maximum velocity of the acoustic streaming is given in the following equation [30,31]:

$$V = \sqrt{2}\pi f a \tag{3}$$

where V is the maximum velocity of the acoustic streaming, f is the frequency of the power ultrasonic field and a is amplitude of vibration. In this study, f is 20 kHz and a is 3.5 μm. The calculated velocity is approximately 0.31 m s^{-1}. Although the actual velocity of the acoustic streaming is smaller than the maximum, it can still cause vigorous stirring of the melt and lead to circumfluence and turbulence of the molten filler metal. The Si and O atoms generated by the decomposition of the SiO_2 film could then diffuse away quickly, leading to the lack of reaction products seen at the interface.

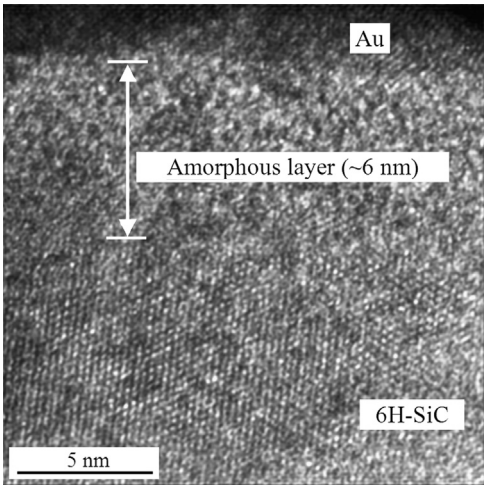

Fig. 6. HRTEM image of the SiC surface that only underwent thermal treatment (420 °C).

The implosion of one cavitation bubble forms an isolated erosion zone. These isolated zones randomize the formation of cavitation bubbles at the interface, making the erosion phenomenon nonuniform. The total number of cavitation bubbles was proportional to the UVDT. Thus, the erosion process of the SiO_2 film was enhanced by prolonging the UVDT. Intuitively, the interfacial bonding strength has an intimate relationship with the degree of erosion, as the strength increased by prolonging the UVDT. Ultrasonic vibration promoted mass transfer from the solid SiO_2 film to the liquid ZnAlMg filler metal, leading to a stronger bond between the ZnAlMg filler metal and the SiC covered by an amorphous SiO_2 film.

4. Conclusion

SiC ceramics were ultrasonic-assisted brazed to each other in air by filling with a ZnAlMg alloy at a low temperature of 420 °C. A strong joint could be obtained using this method. The UVDT had a significant effect on the shear strength of the joint. A maximum shear strength of ~148.1 MPa was achieved when the UVDT was increased to 8 s. An amorphous ~6 nm SiO_2 film formed on the surface of the SiC while heating in air. The SiO_2 film was nonuniformly eroded by the liquid ZnAlMg filler metal in the presence of ultrasonic vibration. The erosion behavior was induced by the impact effects of liquid microjets, shock waves, and localized high temperatures; all of these effects were ascribed to the implosions of cavitation bubbles. Atoms from the eroded SiO_2 film could then diffuse away quickly in the liquid alloy, aided by the acoustic streaming effect. This erosion behavior was described using the cavitation erosion phenomenon. Other amorphous phases not eroded by the liquid ZnAlMg alloy were preserved in the final interface. Strong bonding between the SiC and ZnAlMg could be ascribed to the mass transfer from SiO_2 to ZnAlMg induced by cavitation erosion; this mass transfer behavior was enhanced by prolonging the UVDT.

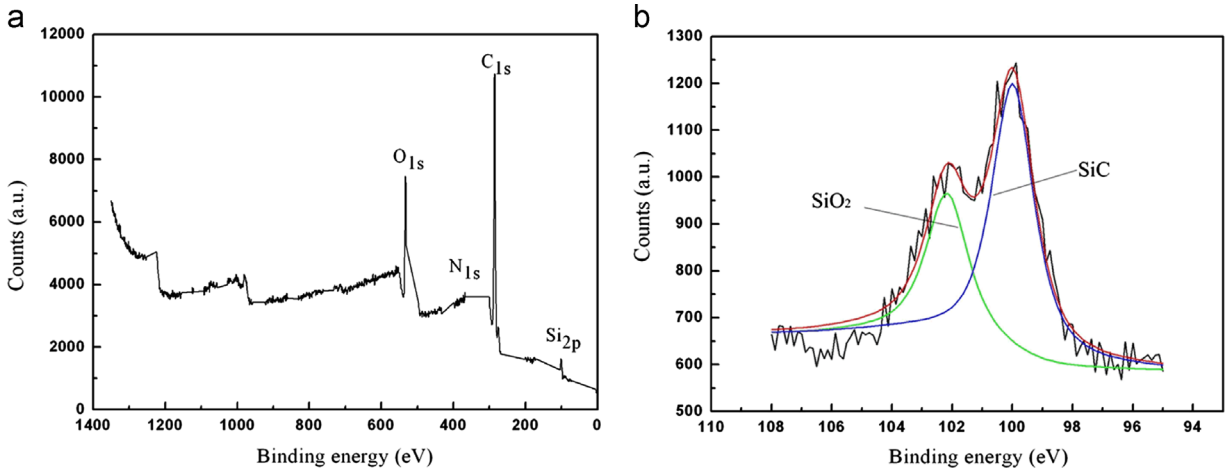

Fig. 7. XPS analysis of the surface of SiC that only underwent thermal treatment (420 °C): (a) typical XPS survey spectrum; and (b) XPS spectrum of the Si 2p core level region.

Acknowledgments

This research was sponsored by the National Natural Science Foundation of China (Grant nos. 50375039 and 51075104).

References

[1] I. Südmeyer, T. Hettesheimer, M. Rohde, On the shear strength of laser brazed SiC-steel joints: effects of braze metal fillers and surface patterning, Ceramics International 36 (2010) 1083–1090.
[2] M.X. Yang, T.S. Lin, P. He, Microstructure evolution of Al_2O_3/Al_2O_3 joint brazed with Ag–Cu–Ti+B+TiH_2 composite filler, Ceramics International 38 (2012) 289–294.
[3] Y. Liu, Z.R. Huang, X.J. Liu, Joining of sintered silicon carbide using ternaty Ag–Cu–Ti active brazing alloy, Ceramics International 35 (2009) 3479–3484.
[4] H.K. Lee, S.H. Hwang, J.Y. Lee, Effects of the relative contents of silver and copper on the interfacial reactions and bond strength in the active brazing of SiC, Journal of Materials Science 28 (1993) 1765–1774.
[5] H.P. Xiong, X.H. Li, W. Mao, Y.Y. Cheng, Wetting behavior of Co based active brazing alloys on SiC and the interfacial reactions, Materials Letters 57 (2003) 3417–3421.
[6] H.P. Xiong, W. Mao, Y.H. Xie, B. Chen, W.L. Guo, X.H. Li, Y. Y. Cheng, Control of interfacial reactions and strength of the SiC/SiC joints brazed with newly-developed Co-based brazing alloy, Journal of Materials Research 22 (2007) 2727–2736.
[7] B. Riccardi, C.A. Nannetti, J. Woltersdorf, E. Pippel, T. Petrisor, Brazing of SiC and SiC_f/SiC composites performed with 84Si–16Ti eutectic alloy: microstructure and strength, Journal of Materials Science 37 (2002) 5029–5039.
[8] J.K. Li, L. Liu, Y.T. Wu, W.L. Zhang, W.B. Hu, A high temperature Ti–Si eutectic braze for joining SiC, Materials Letters 62 (2008) 3135–3138.
[9] J.K. Li, L. Liu, Y.T. Wu, Z.B. Li, W.L. Zhang, W.B. Hu, Microstructure of high temperature Ti-based brazing alloys and wettability on SiC ceramic, Materials Design 30 (2009) 275–279.
[10] M. Naka, H. Taniguchi, I. Okamoto, Heat-resistant brazing of ceramics (report I): brazing of SiC ceramic using Ni–Ti filler metals, Transactions of Japanese Welding Research Institute 19 (1990) 25–31.
[11] Y.H. Chai, W.P. Weng, T.H. Chuang, Relationship between wettability and interfacial reaction for Sn10Ag4Ti on Al_2O_3 and SiC substrates, Ceramics International 24 (1998) 273–279.
[12] R. Koleňák, P. Sebo, M. Provazník, M. Koleňáková, K. Ulrich, Shear strength and wettability of active Sn3.5Ag4Ti(Ge, Ga) solder on Al_2O_3 ceramics, Materials Design 32 (2011) 3997–4003.
[13] S. Tamura, Y. Tsunekawa, M. Okumiya, M. Hatakeyama, Ultrasonic cavitation treatment for soldering on Zr-based bulk metallic glass, Journal of Materials Processing Technology 206 (2008) 322–327.
[14] T. Matsunaga, K. Ogata, T. Hatayama, K. Shinozaki, M. Yoshida, Effect of acoustic cavitation on ease of infiltration of molten aluminum alloys into carbon fiber bundles using ultrasonic infiltration method, Composites: Part A 38 (2007) 771–778.
[15] M. Naka, K.M. Hafez, Applying of ultrasonic waves on the brazing of alumina to copper using Zn–Al filler alloy, Journal of Materials Science 38 (2003) 3491–3494.
[16] M. Naka, M. Maeda, Application of ultrasound on joining of ceramics to metals, Engineering Fracture Mechanics 40 (1991) 951–956.
[17] Y. Zhang, J.C. Yan, X.G. Chen, Y. Cui, Ultrasonic dissolution of brazing of 55% SiC_p/A356 composites, Transactions of the Nonferrous Metals Society of China 20 (2010) 746–750.
[18] Z.W. Xu, J.C. Yan, G.H. Wu, X.L. Kong, S.Q. Yang, Interface structure and strength of ultrasonic vibration liquid phase bonded joints of Al_2O_{3p}/6061Al composites, Scripta Materialia 53 (2005) 835–839.
[19] X.G. Chen, J.C. Yan, S.C. Ren, J.H. Wei, Q. Wang, Ultrasonic-assisted brazing of SiC ceramic to Ti–6Al–4V alloy using a novel AlSnSiZnMg filler metal, Materials Letters 105 (2013) 120–123.
[20] B. Wattiez, A.F. Gourgues, A. Deschamps, A. Roemer, Z. Zermout, Experimental investigation of microstructure and ageing behaviour of bulk Zn–(1–18)wt%Al–(0–0.06)wt%Mg alloys, Materials Science and Engineering: A 527 (2010) 7901–7911.
[21] S.G. Protasova, O.A. Kogtenkova, B.B. Straumal, P. Zieba, B. Baretzky, Inversed solid-phase grain boundary wetting in the Al–Zn system, Journal of Materials Science 46 (2011) 4349–4353.
[22] E.B. Flint, K.S. Suslick, The temperature of cavitation, Science 253 (1991) 1397–1399.
[23] K.S. Suslick, D.A. Hammerton, R.E. Cline, The sonochemical hot spot, Journal of the American Chemical Society 108 (1986) 5641–5642.
[24] E.A. Brujan, Cavitation in Non-Newtonian Fluids, Springer Verlag, Berlin Heidelberg, Romania155–174.
[25] A. Karimi, J.I. Martin, Cavitation erosion of materials, International Metals Reviews 31 (1986) 1–26.
[26] M. Virot, T. Chave, S.I. Nikitenko, D.G. Shchukin, T. Zemb, H. Möhwald, Acoustic cavitation at the water–glass interface, Journal of Physical Chemistry C 114 (2010) 13083–13091.
[27] D.G. Shchukin, E. Skorb, V. Belova, H.H. Möhwald, Ultrasonic cavitatiion at solid surface, Advanced Materials 23 (2011) 1922–1934.
[28] P. Shen, H. Fujii, T. Matsumoto, K. Nogi, Reactive wetting of SiO_2 substrates by molten Al, Metallurgical and Materials Transactions A 35 (2004) 583–588.
[29] I. Gutman, L. Klinger, I. Gotman, M. Shapiro, Experimental observation of periodic structure formation in SiO_2–Mg system, Scripta Materialia 45 (2001) 363–367.
[30] X.G. Chen, J.C. Yan, F. Gao, J.H. Wei, Z.W. Xu, G.H. Fan, Interaction behaviors at the interface between liquid Al–Si and solid Ti–6Al–4V in ultrasonic-assisted brazing in air, Ultrasonics Sonochemistry 20 (2013) 144–154.
[31] J. Campbell, Effect of vibration during solidification, International Metals Reviews 26 (1981) 71–108.